CrossMark

Characterization of CuO–reduced graphene oxide sandwiched nanostructure and its hydrogen sensing characteristics

Dongzhi Zhang[1] · **Nailiang Yin**[1] · **Chuanxing Jiang**[1] · **Bokai Xia**[1]

Abstract This paper demonstrated a high-performance hydrogen gas sensor based on CuO–reduced graphene oxide (rGO)–CuO sandwiched nanostructure. The CuO–rGO–CuO nanostructure was examined by scanning electron microscopy, X-ray diffraction and transmission electron microscope. The gas sensing characteristics of the CuO–rGO–CuO film sensor were evaluated at room temperature against hydrogen over a wide concentration range, which are better than that of pristine CuO and rGO. High sensitivity, good repeatability, and response–recovery characteristics were achieved in this work. Furthermore, the possible sensing mechanism of the presented sensor was explored.

1 Introduction

Hydrogen gas has been widely used as a clean fuel in many fields. Since hydrogen is highly inflammable, colorless and odorless, its leakage can lead to potential explosion risks at concentrations beyond 4 vol. % in ambient air [1]. Therefore, portable, reliable, high-precision and low-cost hydrogen sensors are highly desired. Many researchers have made a lot of efforts to develop high-performance hydrogen sensors [2–10]. Currently, gas chromatography in the laboratory can achieve off-line monitoring but hard to realize on-line monitoring [11, 12]. On-line real-time monitoring methods such as photo acoustic spectrometry [13] and infrared spectrometry [14, 15], were limited because the acquired weak signals are easy to be influenced. Recently, gas sensors based on metal oxide semiconductor are reported for gas detection on account of their unique advantages including smaller size, lower power consumption, high sensitivity, relative selectivity, reproducibility, reliability, and simplicity of use [16–20]. Zhang et al. [21] fabricated platinum-activated tungsten oxide (Pt–WO₃) films for highly sensitive hydrogen sensors, and the sensing properties were tested against 30–200 ppm H_2 in air at temperatures varied from 95 to 220 °C. Sanhita et al. [22] reported a carbon nanotube/SnO_2 thin film-based hydrogen sensor working at an optimum temperature of 200 °C. Kanika et al. [23] found that graphene/ZnO nanocomposite showed an outstanding behavior in hydrogen detection, while the operating temperature reaches to 150 °C. However, some sensors exhibited a prolonged response and recovery in hydrogen sensing and some exhibited a narrow scope of testing and low sensitivity.

Copper oxide (CuO) is a semiconductor with a band gap of about 1.2–1.9 eV, and it has been reported to be suitable for catalysis [24], electrochemical cells [25], field emission device [26], and gas sensor application [27]. It has been found that nanoparticles, nanoribbons, plates, and nanowires of CuO are sensitive to formaldehyde, ethanol and H_2S [28–30]. Graphene has attracted the attention of sensor community owing to its unique nanostructure, excellent physical and chemical properties [31, 32]. Among graphene derivatives, graphene oxide (GO) and reduced graphene oxide (rGO) have triggered considerable attention due to their facile preparation and novel applications [33, 34]. In this work, we demonstrated a CuO–rGO–CuO sandwiched film-based hydrogen sensor. The as-prepared film was inspected by SEM, XRD and TEM measurement. The presented sensor achieved high-

✉ Dongzhi Zhang
  dzzhang@upc.edu.cn

1 College of Information and Control Engineering, China University of Petroleum (East China), Qingdao 266580, China

performance properties toward hydrogen sensing. And finally, the underlying sensing mechanism of the sensor was discussed in detail.

2 Experiment

2.1 Sample preparation

CuO nanorods were synthesized by a facile hydrothermal method. 0.17 g $CuCl_2 \cdot 2H_2O$ and 0.11 g Na_2CO_3 were dissolved in 40 mL deionized water and been stirred for 1 h. And then, the resulting solution was thermally treated at 180 °C for 18 h. The CuO solution was collected by the process of centrifugation, water washing and ultrasonication. CuO was produced in terms of the reaction described by $2CuCl_2 + 2Na_2CO_3 + H_2O \rightarrow 2CuO + 2CO_2 + 4NaCl$. During the fabrication of sensing film, the alternative deposition of CuO and GO was performed in solution. Figure 1 shows the structure of the sensor with electrodes and sensing film deposited on substrate. In this work, two sensors with structures of three-layer CuO–GO–CuO, five layer $(CuO–GO)_2$–CuO were fabricated, another two sensors coated with pure GO and CuO film were fabricated by drop-casting suspension on the substrate. The sensor samples were heated at 180 °C for 3 h in order to convert GO into rGO through removing the oxygen-containing groups. The four samples were employed to investigate their sensing properties and make comparisons.
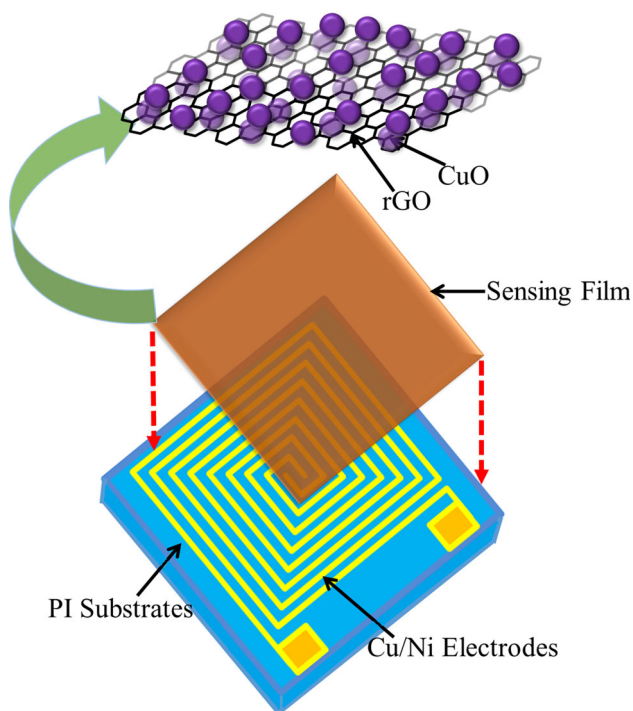
Fig. 1 Structure illustration of hydrogen sensor

2.2 Instrument and analysis

The surface micromorphology of the CuO–rGO–CuO film was inspected with a field emission scanning electron microscopy (Hitachi S-4800). X-ray diffraction (XRD) spectrum was measured by an X-ray diffractometer (Rigaku D/Max 2500PC). The nanostructure of the as-prepared samples was observed by a transmission electron microscope (TEM; JEOL JEM-2100, Japan).

The schematic of the experimental setup for hydrogen gas-sensing is shown in Fig. 2. The measurement was performed at room temperature and relative humidity of 55 % RH. The sensing properties were investigated by exposing the sensor to various concentrations of hydrogen gas. The desired gas concentration was obtained by injecting a required quantity of hydrogen into a sealed glass chamber using a syringe. The sensitivity of the sensor was defined as $S = (R_0 - R_g)/R_0 \times 100 \%$, where R_0 and R_g were the sensor resistance in dry air and hydrogen gas, respectively. The time taken by a sensor to achieve 90 % of the total resistance change is defined as the response or recovery time and each exposure/recovery cycle was carried out by an exposure interval of 200 s, followed by a recovery interval of 200 s at dry air.

3 Results and discussion

3.1 SEM and XRD characterization

The SEM images of CuO, rGO and CuO/rGO samples are shown in Fig. 3. Figure 3a clearly shows the CuO has a
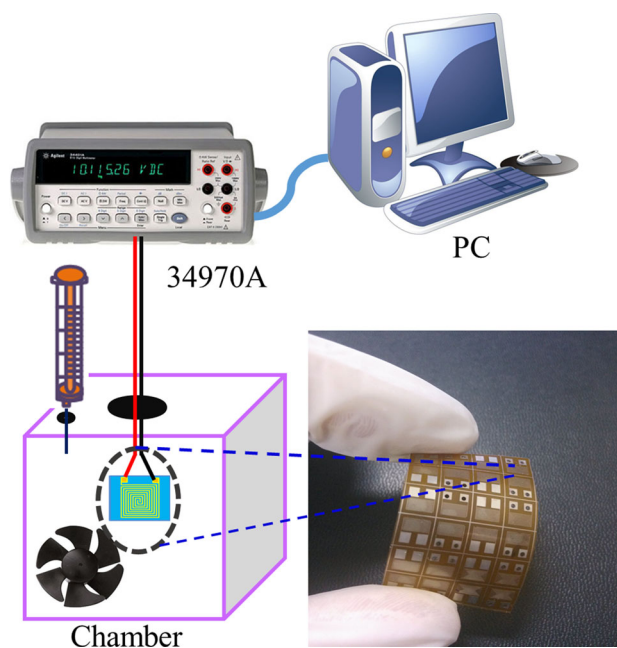
Fig. 2 Schematic of hydrogen sensing experimental setup

nanorod shape. Figure 3b shows that rGO has pleated shape. Figure 3c shows CuO and rGO has good contact in the CuO/rGO hybrid and form porous nanostructure.

Figure 4 plots the XRD spectrum for CuO, rGO and CuO/rGO samples. XRD of the CuO shows the major peaks attributed to the (002) and (111) planes of CuO
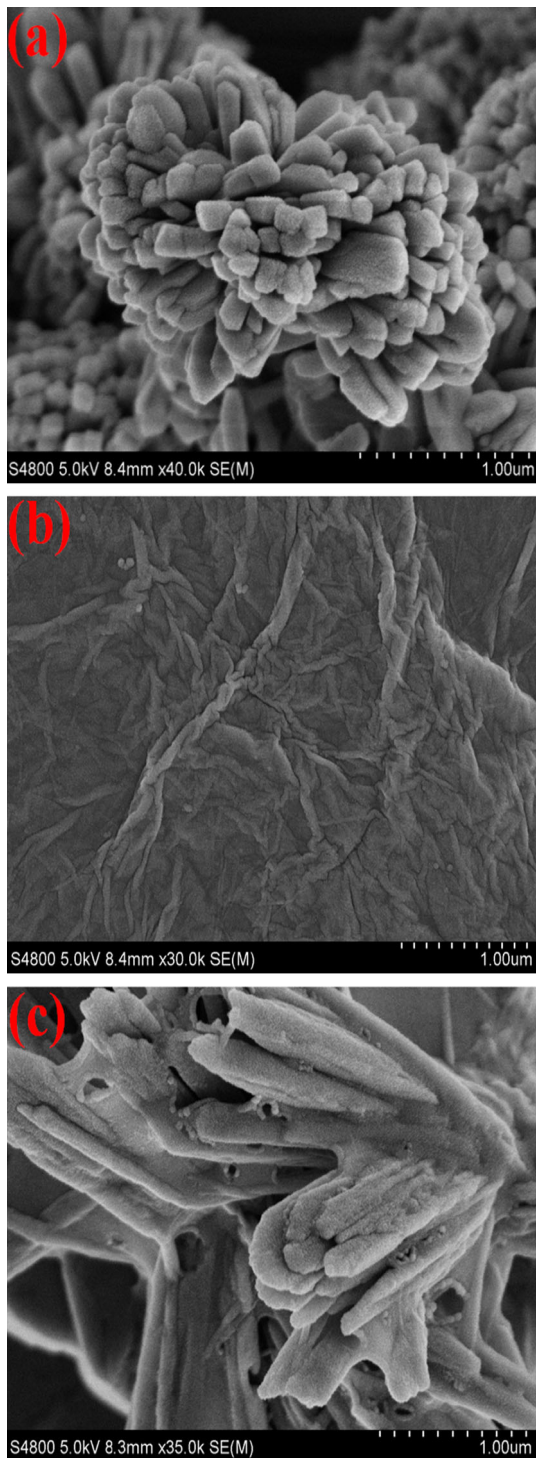
polycrystallines. The spectrum of rGO exhibits a wide diffraction peak at 24.73° [34]. The featured peaks attributed to the CuO and rGO are both present in the XRD pattern for CuO/rGO samples.

In order to confirm the crystallinity of CuO on the rGO surface, TEM and HRTEM images were shown in Fig. 5. Figure 5a, b illustrate the TEM images of CuO/rGO sample, in which the nanorod-shape CuO and nanosheet-shape rGO can be clearly observed. Figure 5c shows the high resolution TEM image of rGO fringes with a spacing distance of 0.34 nm, attributing to the (002) plane of rGO. Figure 5d shows the fringes spacing of 0.22 nm, corresponding to the (200) plane of the CuO.

3.2 Hydrogen-sensing properties

The hydrogen-sensing properties of the four sensors with CuO–rGO–CuO, $(CuO–rGO)_2$–CuO, pure rGO and CuO as sensing film were investigated. The measurement was performed by exposing the sensors to various hydrogen concentrations ranging from 50 to 1500 ppm. Figure 6 plots the sensor sensitivity as a function of hydrogen gas concentration for the four sensors. Here, S_1, S_2, S_3 and S_4 are labeled to represent the four sensors based on CuO–rGO–CuO, $(CuO–rGO)_2$–CuO, rGO and CuO, respectively. The fitting curves for the sensitivity Y and gas concentrations X can be represented as $Y = 4.14 - 3.35e^{(-X/1477)}$, $Y = 12.24 - 10.77e^{(-X/558)}$, $Y = 11.34 - 9.91e^{(-X/1174)}$ and $Y = 7.29 - 6.40e^{(-X/578)}$ for S1, S2, S3, and S4, respectively, and the linear regression coefficient, R^2, is 0.90319, 0.95333, 0.99181, 0.96786, respectively. From the experimental results shown in Fig. 6, we found that the sensor S_1 based on CuO–rGO–CuO film achieved the highest sensitivity among the four samples, and hence the sensor S1 was selected to perform the subsequent investigation for hydrogen sensing.

Fig. 3 SEM characterization of a CuO, b rGO, c CuO/rGO samples
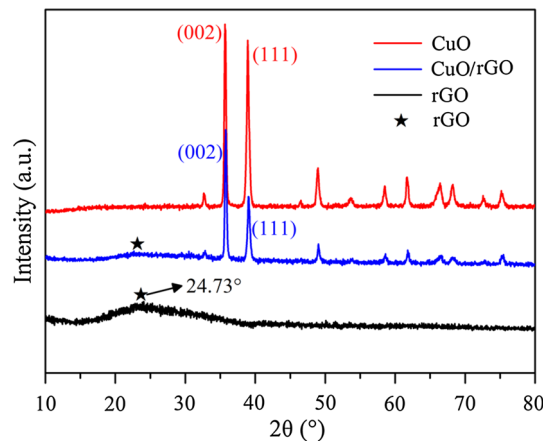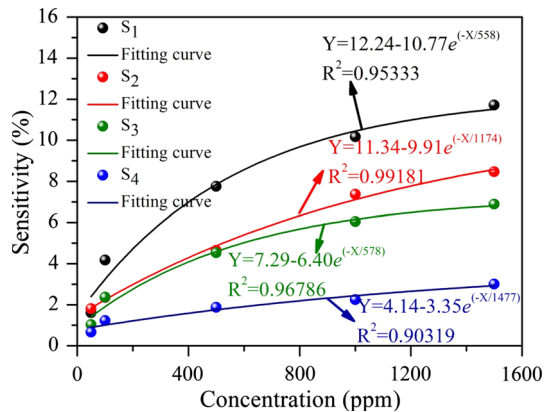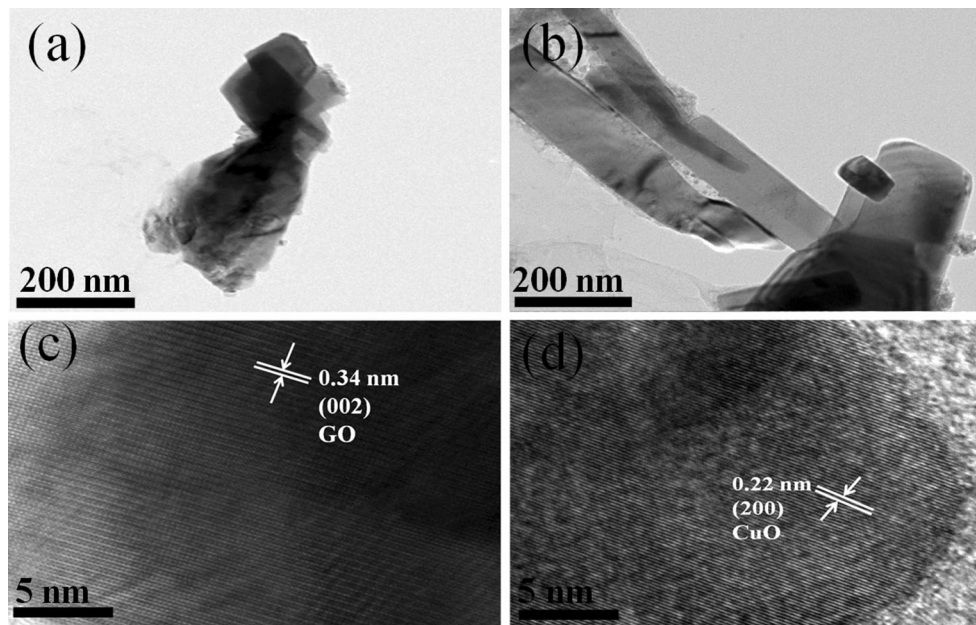

Fig. 4 XRD spectrum of CuO, rGO, CuO/rGO samples

Fig. 5 TEM images of **a** and **b** CuO/rGO sample, HRTEM images of **c** rGO fringe and **d** CuO/rGO sample
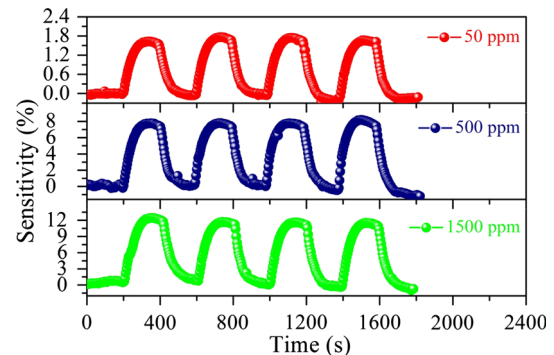

Fig. 6 The sensor sensitivity as a function of hydrogen gas concentration for four sensors

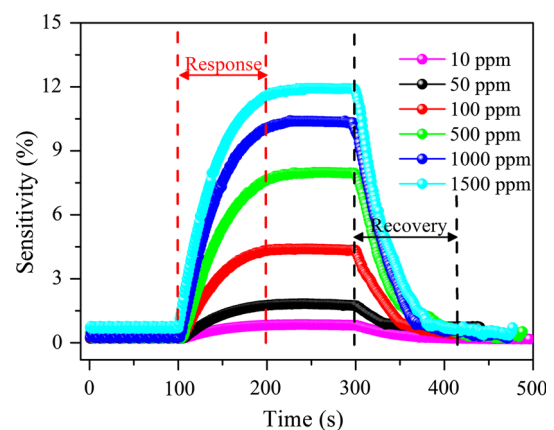**Fig. 7** Repeatability of the CuO–rGO–CuO film sensor toward 50, 500 and 1500 ppm hydrogen gas

Figure 7 shows the repeatability of the CuO–rGO–CuO film sensor, which was measured for four exposure/recovery cycles repeatedly upon exposure to 50, 500 and 1500 ppm of hydrogen. The sensor exhibited a good response–recovery behavior and acceptable repeatability for hydrogen sensing. Figure 8 demonstrates the time-dependent response and recovery curves of the sensor toward hydrogen pulse from 0 to 10, 50, 100, 500, 1000 and 1500 ppm. Response time and recovery time of less than 80 and 60 s are observed.

3.3 Hydrogen-sensing mechanism

The as-prepared CuO–rGO–CuO hybrid film sensor exhibited an excellent response and short response/recovery characteristics toward hydrogen detection at room temperature, which may be attributed to the synergistic

Fig. 8 Response–recovery curves of the CuO–rGO–CuO film sensor toward hydrogen gas with various concentrations

effects between CuO and graphene. CuO is a typical p-type semiconductor with excellent physiochemical properties, and serve as surface catalytically active centers toward gas

molecules. Graphene acts as a conducting layer for electron transfer with low noise and high mobility. CuO nanorods can efficiently prevent the aggregation of rGO nanosheets, and generate much more active sites and form porous structure as shown in SEM images of Fig. 3c, all of which facilitate adsorption and diffusion of hydrogen gas molecules, resulting in improving the sensing characteristics in terms of high response/recovery speeds. A hole accumulation layer will be formed at the heterojunction interface of CuO–rGO–CuO nanostructure. The electrical conductance of the CuO–rGO–CuO film is determined by the amount of holes in its conduction band. The pre-adsorbed oxygen on the CuO surface will be ionized to O_2^- through trapping electron from the conduction band of CuO, as depicted in Eqs. (1)–(2) [35, 36]. When the sensor is exposed to hydrogen molecules, the adsorbed hydrogen interacts with the oxygen species and products water molecules and free electrons according to Eqs. (3)–(4) [37, 38]. The illustration of sensing mechanism of the CuO–rGO–CuO film is shown in Fig. 9. Hydrogen adsorbed at the sensing film led to electronic sensitization by modulating the accumulation layers by donation of electron. Hence, the electron–hole recombination in the hole accumulation layer results in the change of sensor resistance.

$$O_2(gas) \rightarrow O_2(ads) \tag{1}$$

$$O_2(gas) + e^- \rightarrow O_{2-}(ads) \tag{2}$$

$$H_2(gas) \rightarrow H_2(ads) \tag{3}$$

$$2H_2(ads) + O_{2-}(ads) \rightarrow 2H_2O + e^- \tag{4}$$
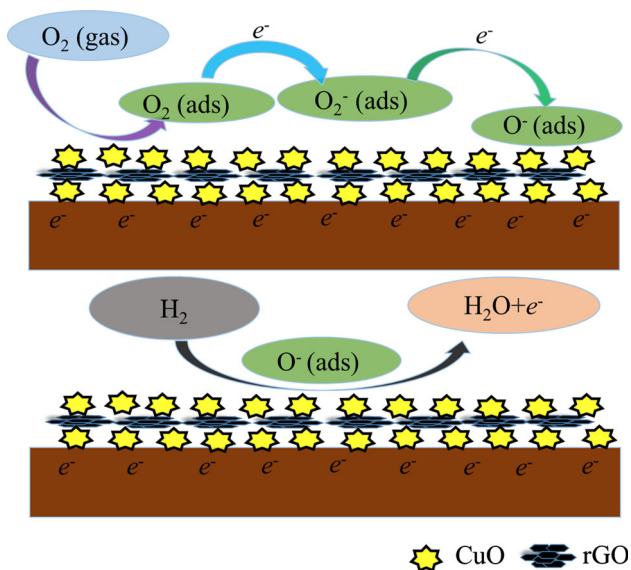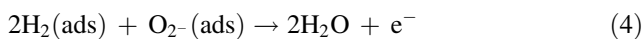
The sensitivity of CuO–rGO–CuO film against hydrogen sensing is higher than that of pure CuO, rGO and (CuO–rGO)$_2$–CuO samples in this work. This is because the conductivity of CuO is much lower, and the ability of rGO in capturing hydrogen molecule is weaker than the CuO–rGO–CuO hybrid film. The thickness of (CuO–rGO)$_2$–CuO film is much larger than that of CuO–rGO–CuO, the obtained electrons may be disappeared into oblivion during the process of multi-layer transfer, and thus result in a weaker performance than CuO–rGO–CuO film.

4 Conclusions

In summary, we prepared a sandwiched CuO–rGO–CuO film for fabricating hydrogen gas sensor. The sensing film was characterized by SEM and XRD. The sensing properties of the film sensor toward hydrogen gas was investigated at room temperature, exhibiting a swift response-recovery characteristic and outstanding stability upon exposure to different concentration of hydrogen. Finally, the possible mechanism for hydrogen sensing was discussed. This work provides an alternative way for the fabrication of hydrogen sensor based on CuO–rGO–CuO film.

Compliance with ethical standards

Conflict of interest The authors declared that they have no conflicts of interest to this work.

Fig. 9 Illustration of sensing mechanism of the CuO–rGO–CuO film sensor

References

1. P.A. Pandey, N.R. Wilson, J.A. Covington, Pd-doped reduced graphene oxide sensing films for H$_2$ detection. Sens. Actuators B Chem. **183**, 478–487 (2013)
2. J. Hong, S. Lee, J. Seo, S. Pyo, J. Kim, T. Lee, A highly sensitive hydrogen sensor with gas selectivity using a PMMA membrane-coated Pd nanoparticle/single-layer graphene hybrid. ACS Appl. Mater. Interfaces **7**, 3554–3561 (2015)
3. D. Dutta, S.K. Hazra, J. Das, C.K. Sarkar, S. Basu, Studies on p-TiO$_2$/n-graphene heterojunction for hydrogen detection. Sens. Actuators B Chem. **212**, 84–92 (2015)
4. Y. Lim, Y. Lee, J. Heo, H. Shin, Highly sensitive hydrogen gas sensor based on a suspended palladium/carbon nanowire fabricated via batch microfabrication processes. Sens. Actuators B Chem. **210**, 218–224 (2015)
5. Y.R. Wang, B. Liu, S.H. Xiao, H. Li, L.L. Wang, D.P. Cai, D.D. Wang, Y. Liu, Q.H. Li, T.H. Wang, High performance and

negative temperature coefficient of low temperature hydrogen gas sensors using palladium decorated tungsten oxide. J. Mater. Chem. A **3**, 1317–1324 (2015)

6. M. Darabpour, M. Doroodmand, Fabrication of a glow discharge plasma-based ionization gas sensor using multiwalled carbon nanotubes for specific detection of hydrogen at parts per billion levels. IEEE Sens. J. **15**, 2391–2398 (2015)

7. B. Wang, Z.Q. Zheng, L.F. Zhu, Y.H. Yang, H.Y. Wu, Self-assembled and Pd decorated Zn_2SnO_4/ZnO wire-sheet shape nano-heterostructures networks hydrogen gas sensors. Sens. Actuators B Chem. **195**, 549–561 (2014)

8. R. Abkadir, Z.Y. Li, A. Sadek, R. Abdulrani, A. Zoolfakar, M. Field, J.Z. Qu, A. Chrimes, K. Kalantar-Zadeh, Electrospun granular hollow SnO_2 nanofibers hydrogen gas sensors operating at low temperatures. J. Phys. Chem. C **118**, 3129–3139 (2014)

9. B. Mondal, B. Basumatari, J. Das, C. Roychaudhury, H. Saha, N. Mukherjee, ZnO–SnO_2 based composite type gas sensor for selective hydrogen sensing. Sens. Actuators B Chem. **194**, 389–396 (2014)

10. D. Jung, M. Han, G.S. Lee, Gas sensor using a multi-walled carbon nanotube sheet to detect hydrogen molecules. Sens. Actuators A Phys. **211**, 51–54 (2014)

11. E. Christine, B. Peter, W. Friedrich, S. Torsten, Multi- component trace analysis of organic xenobiotics in surface water containing suspended particular matter by solid phase extraction/gas chromatography-mass spectrometry. J. Chromatogr. A **1249**, 181–189 (2012)

12. C.H. Wang, S.W. Chiang, J.L. Wang, Simultaneous analysis of atmospheric halocarbons and non-methane hydrocarbons using two-dimensional gas chromatography. J. Chromatogr. A **3**, 353–358 (2010)

13. A. Grossel, V. Zéninari, B. Parvitte, L. Joly, D. Courtois, Optimization of a compact photoacoustic quantum cascade laser spectrometer for atmospheric flux measurements: application to the detection of methane and nitrous oxide. Appl. Phys. B **88**, 483–492 (2007)

14. B. Mortazavi, B.J. Wilson, F. Dong, M. Gupta, D. Baer, Validation and application of cavity-enhanced, near-infrared tunable diode laser absorption spectrometry for measurements of methane carbon isotopes at ambient concentrations. Environ. Sci. Technol. **47**, 11676–11684 (2013)

15. H. Abdul, B.C. Morat, R. Abdul, Non-invasive evaluation of hydrogen peroxide concentrations in a drinking bottle by near-infrared spectrometry. Sens. Transducers **131**, 83–90 (2011)

16. D. Zhang, A. Liu, H. Chang, B. Xia, Room-temperature high-performance acetone gas sensor based on hydrothermal synthesized SnO_2-reduced graphene oxide hybrid composite. RSC Adv. **5**, 3016–3022 (2015)

17. C. Liewhiran, N. Tamaekong, A. Wisitsoraat, A. Tuantranont, S. Phanichphant, Ultra-sensitive H_2 sensors based on flame-spray-made Pd-loaded SnO_2 sensing films. Sens. Actuators B Chem. **176**, 893–905 (2013)

18. D. Zhang, H. Chang, P. Li, R. Liu, Characterization of nickel oxide decroated-reduced graphene oxide nanocomposite and its sensing properties toward methane gas detection. J. Mater. Sci. Mater. Electron. **27**, 3723–3730 (2016)

19. F. Bayata, B. Saruhan-Brings, M. Ürgen, Hydrogen gas sensing properties of nanoporous Al-doped titania. Sens. Actuators B Chem. **204**, 109–118 (2014)

20. D. Zhang, N. Yin, B. Xia, Y. Sun, Y. Liao, Z. He, S. Hao, Humidity-sensing properties of hierarchical ZnO/MWCNTs/ZnO nanocomposite film sensor based on electrostatic layer-by-layer self-assembly. J. Mater. Sci. Mater. Electron. **27**, 2481–2487 (2016)

21. C. Zhang, A. Boudiba, C. Navio, C. Bittencourt, M.G. Olivier, R. Snyders, M. Debliquy, Highly sensitive hydrogen sensors based on co-sputtered platinum activated tungsten oxide films. Int. J. Hydrog. Energy **36**, 1107–1114 (2011)

22. M. Sanhita, N. Pratanu, S.D. Parukuttyamma, Enhanced performance of CNT/SnO_2 thick film gas sensors towards hydrogen. Mater. Chem. Phys. **147**, 79–85 (2014)

23. A. Kanika, S. Onkar, P.S. Manmeet, Hydrogen sensor based on graphene/ZnO nanocomposite. Sens. Actuators B Chem. **195**, 409–415 (2014)

24. K. Zhou, R. Wang, B. Xu, Y. Li, Synthesis, characterization and catalytic properties of CuO nanocrystals with various shapes. Nanotechnology **17**, 3939–3943 (2006)

25. L.B. Chen, N. Lu, C.M. Xu, H.C. Yu, T.H. Wang, Electrochemical performance of polycrystalline CuO nanowires as anode material for Li ion batteries. Electrochim. Acta **54**, 4198–4201 (2009)

26. Y.W. Zhu, T. Yu, F.C. Cheong, X.J. Xu, C.T. Lim, V.B.C. Tan, J.T.L. Thong, C.H. Sow, Large-scale synthesis and field emission properties of vertically oriented CuO nanowire films. Nanotechnology **16**, 88–92 (2005)

27. J. Zhang, J. Liu, Q. Peng, X. Wang, Y. Li, Nearly monodisperse Cu_2O and CuO nanospheres: preparation and applications for sensitive gas sensors. Chem. Mater. **18**, 867–871 (2006)

28. H.J. Park, N.J. Choi, H. Kang, M.Y. Jung, J.W. Park, K.H. Park, D.S. Lee, A ppb-level formaldehyde gas sensor based on CuO nanocubes prepared using a polyol process. Sens. Actuators B Chem. **203**, 282–288 (2014)

29. A. Taubert, F. Stange, Z.H. Li, M. Junginger, C. Gunter, M. Neumann, A. Friedrich, CuO nanoparticles from the strongly hydrated ionic liquid precursor (ILP) tetrabutyl ammonium hydroxide: evaluation of the ethanol sensing activity. ACS Appl. Mater. Interfaces **4**, 791–795 (2012)

30. S. Steinhauer, E. Brunet, T. Maier, G.C. Mutinati, A. Kock, Suspended CuO nanowires for ppb level H_2S sensing in dry and humid atmosphere. Sens. Actuators B Chem. **186**, 550–556 (2013)

31. D. Zhang, H. Chang, P. Li, R. Liu, Q. Xue, Fabrication and characterization of an ultra-sensitive humidity sensor based on metal oxide/graphene hybrid nanocomposite. Sens. Actuators B Chem. **225**, 233–240 (2016)

32. R. Furue, E.P. Koveke, S. Sugimoto, Y. Shudo, S. Hayami, S.I. Ohira, K. Toda, Arsine gas sensor based on gold-modified reduced graphene oxide. Sens. Actuators B Chem. **240**, 657–663 (2017)

33. D. Zhang, J. Tong, B. Xia, Q. Xue, Ultrahigh performance humidity sensor based on layer-by-layer self-assembly of graphene oxide/polyelectrolyte nanocomposite film. Sens. Actuators B Chem. **203**, 263–270 (2014)

34. D. Zhang, J. Tong, B. Xia, Humidity-sensing properties of chemically reduced graphene oxide/polymer nanocomposite film sensor based on layer-by-layer nano self-assembly. Sens. Actuators B Chem. **197**, 66–72 (2014)

35. Y. Kwon, H. Kim, S. Lee, I.J. Chin, T.Y. Seong, W.I. Lee, C. Lee, Enhanced ethanol sensing properties of TiO_2 nanotube sensors. Sens. Actuators B Chem. **173**, 441–446 (2012)

36. D.H. Nguyen, Y.A. Sea, Q.D. Nguyen, V.Q. Nguyen, K. Dojin, Synthesis of p-type semiconducting cupric oxide thin films and their application to hydrogen detection. Sens. Actuators B Chem. **146**, 239–244 (2010)

37. Z. Zhang, X. Zou, L. Xu, L. Liao, W. Liu, J. Ho, X. Xiao, C. Jiang, J. Li, Hydrogen gas sensor based on metal oxide nanoparticles decorated graphene transistor. Nanoscale **7**, 10078–10084 (2015)

38. I.H. Kadhim, H.A. Hassan, Room temperature hydrogen gas sensor based on nanocrystalline SnO_2 thin film using sol–gel spin coating technique. J. Mater. Sci. Mater. Electron. **27**, 4356–4362 (2016)